A TWO-CHANNEL MONOPULSE TELEMETRY AND TRACKING ANTENNA FEED

R. R. YAMINY
Senior Engineer
RIF Department
Radiation Systems, Inc.

Summary The two-channel monopulse telemetry and tracking antenna feed operates over the frequency range from 1435 to 2300 MHz. The feed was designed and developed for a 7-foot parabolic reflector located in the nose cone of an EC-135N aircraft. This airborne system maintains in-flight voice and telemetry communications with Apollo spacecraft during the injection and reentry phases of the Apollo missions.

The feed consists of a planar multimode dual-polarized cavity-backed spiral radiator and two printed circuit comparators. The spiral radiator is excited in the sum and difference modes at both its inner and outer filament terminals. This allows the simultaneous reception of right-hand and lefthand circularly polarized signals. The sum and difference modes of excitation are precisely controlled to provide the proper reflector illumination functions for improved sidelobes and efficiency. Sidelobe levels in excess of 22 db, null depths greater than 40 db, boresight shifts of less than 0.25 degree, and system efficiencies of greater than 40 percent have been achieved.

Introduction The feed system discussed in this paper was developed for operation aboard an EC-135N instrumented aircraft for the Apollo Moon (A/RIA)[1] project. The feed's prime object is to provide the proper sum and difference pattern illumination functions for a 7-foot parabolic reflector.

The feed system is an integral assembly consisting of a 6-arm spiral radiator and two stripline excitation networks. The spiral radiator is a six-arm cavity-backed planar log-periodic spiral. The spiral element arms are fed from both the inner terminal ends and the outer terminal ends. This excitation method results in an antenna feed which is simultaneously dual circularly polarized (RHC and LHC). The six-port excitation network is a stripline printed circuit board which consists of quadrature couplers and fixed 90-degree phase shifters. This comparator circuit is preferred because coupled

[1] Apollo Range Instrumented Aircraft.

transmission line couplers can be easily fabricated in stripline configuration and the dielectric employed is irradiated polyolefin which has very low loss.

Attention will be directed to the basic theory of operation of the twochannel monopulse feed technique. Advantages of this system over the conventional three-channel systems will be outlined. This paper will also describe the technique utilized for the design of the dual-polarized feed along with its performance characteristics.

The Basic Two-Channel Monopulse Concept Figure 1 illustrates two types of monopulse systems. Figure 1(a) depicts the conventional three-channel monopulse arrangement in which a hybrid feed network attached to the radiator system provides three RF outputs; a sum, a difference elevation, and a difference azimuth. Each of these three outputs is fed through a receiver and the sum is compared with each of the differences to provide elevation and azimuth error outputs. In Figure l(b) the same radiator and hybrid feed network are used. However, the two difference outputs are combined in phase quadrature to give a single complex difference channel. The resulting two channels are fed through receivers. The sum and difference outputs are processed by two phase demodulators to provide azimuth and elevation error information.

A practical method of combining the elevation and azimuth difference channel into a single complex difference channel is a 90-degree phase shift hybrid junction. This transformation results in two complex difference channels and one that is the complex conjugate of the other. The basic distinction between the three-channel and the two-channel systems is that in the three-channel system both the azimuth and elevation difference channels are required to obtain tracking information, whereas, in the two-channel system the same information is provided in each of the error channels. Thus, in the two-channel system one of the error channels can be discarded without loss of information.

The far-field pattern characteristics which typify the two-channel monopulse technique are illustrated in the amplitude and phase plot of Figure 2. The sum pattern is identical to that of the three-channel monopulse system. The two-channel difference pattern resembles that of its three-channel counterpart with the exception that it is symmetric about the boresight axis. Hence, while the three-channel system has planar nulls in its azimuth and elevation planes, the two-channel system has a point null and only one difference pattern. One further distinguishing characteristic of the complex two-channel difference pattern is its phase variation. The far-field relative phase between the sum and difference patterns varies through 360 degrees as the angle about the boresight axis varies through the same range. It is these complete amplitude and phase characteristics of the difference pattern which allow the elimination of the third channel needed in the conventional monopulse system. The difference in the signal intensity between the sum

and difference channels defines the angular offset from the boresight position. The relative phase difference between the sum and difference patterns defines the position of the target relative to the vertical or horizontal reference axis.

Feed System Design The antenna feed system for monopulse operation is composed of two basic components; the antenna feed radiator and the necessary feed networks to excite the required sum and difference modes. Several configurations can be utilized as the antenna feed radiators. These range from the simplest to the most complex with complete aperture control. Some of these configurations are shown in Figure 3.

The uppermost aperture configuration represents the commonplace fourhorn cluster. Unfortunately, although this four-horn cluster represents the simplest of the aperture configurations, it also allows little control over the sum and difference illumination. The array factor for this arrangement is such that the maximum of the difference pattern is coincident with the first null of the sum pattern. Consequently, the difference pattern is generally inefficient and often characterized by high sidelobes.

The second approach, illustrated in Figure 3, is a five-horn cluster with four horns oriented around the center aperture. With this configuration the sum and difference illuminations at the edge of the reflector can be equated; however, the difference pattern is now characterized by high sidelobe levels. These sidelobe levels exist by virtue of the increased spacing between the individual elements.

The third arrangement consists of a series of concentric ring apertures. Separate control can be exercised over the excitation coefficient for both the sum and difference modes. This ring aperture allows complete and independent control of the sum and difference pattern. Unfortunately, the excitation networks for this type of structure would be extremely complex.

The final arrangement represents the first two modes that can be radiated by a multi-arm planar spiral. The multi-arm spiral is a radiator that best approximates a series of concentric apertures. It is capable of providing circularly polarized signals, the sense of which is defined by the physical sense of the spiral windings. One sense can be achieved by exciting the structure at its center feed points. The opposite sense can simultaneously be achieved by exciting the spiral at its outer (or peripheral) feed points.

The first mode, or sum mode, radiates from a circumference of approximately one wavelength. The second mode, or complex difference mode, radiates from a circumference of approximately two wavelengths. The resulting feed patterns are circularly symmetric and, hence, are ideal for illuminating a reflector having a circular aperture. Reflector edge illumination can be precisely controlled; therefore, antenna temperature, sidelobes, gain, and efficiency can be optimized. The difference mode of

excitation (mode 2) is excited at a diameter on the planar spiral which is twice the diameter of which the sum mode (mode 1) is excited. As a consequence, the primary difference aperture is twice as large as the sum aperture and the primary difference pattern falls inside the envelope of the primary sum pattern main lobe. This allows the edge illumination for both modes to be equated.

The complexity of the design of the required excitation networks for a spiral radiator depends on the number of spiral arms to be excited. These networks must provide the proper amplitude distribution and phase progression to generate the sum and difference modes. Figure 4 is a block diagram of a six-port comparator network. It is composed of five 3-db quadrature couplers, two 4.78-db couplers, and three fixed 90-degree phase shifters. This matrix configuration provides equal amplitude distribution to all six spiral arms but with a progressive phase, as shown in the bottom of Figure 4. For a six-arm structure, the sum mode is excited by feeding adjacent arms with a 60-degree relative phase differential. To excite the difference mode, adjacent arms are fed with a 120-degree relative phase differential and opposite arms are fed in phase. There is one advantage to this six-port matrix design. It has a plane of symmetry and, as a consequence, is composed of two identical three-port networks that utilize identical subcomponents. This, in turn, offsets any phase or amplitude deviations that are inherent in the design of the couplers and the phase shifters, which results in balanced excitation at the spiral arms.

Feed Component Description The two-channel monopulse feed system being described in this paper is shown in Figure 5. The spiral radiator consists of six spiral arms photoetched on the surface of a copper-clad Teflon-fiberglass sheet. The spiral surface is supported at its center by the center feed tube. The periphery is supported by an angle ring fastened to the cavity. The two stripline excitation networks are mounted parallel to the back of the cavity base by aluminum supports. The two networks are identical. One is used to excite the inner feed points of the spiral arms, thus providing one sense of circular polarization; the other is used to excite the outer feed points of the spiral arms, thus providing the other sense of circular polarization. It should be remarked here that the input impedance of the spiral arms is not the same for inner and outer feeding and that the spiral arms/coaxial feed line interface junction has built into it a tapered flare angle ring that serves as an impedance matching section and a wave launcher. This technique was very successful and individual spiral arm VSWR’s of less than 1.7:1 were achieved for both the inner and outer feed points over the entire 1435 to 2300 MHz band.

One of the basic advantages of strip-transmission line is the ease of designing and packaging many TEM coupled components into a single assembly with no interconnections. Such configurations are ideal for hybrid networks, such as the six-port monopulse comparator developed for this system, in which phase and amplitude must be

carefully controlled. Figure 6 is a photograph of the center layer of the excitation network. The basic material is copper-clad irradiated polyolefin which is etched by a photo-chemical process to produce the basic network components such as couplers and phase shifters. The center board is further sandwiched between two irradiated polyolefin dielectric sheets which are aluminum-backed on one side. The aluminum backing serves as the groundplane required for the strip-transmission-line package.

Feed System Performance Figure 7 shows typical sum and difference patterns of the feed when the spiral arms are excited from their inner terminal points. Figure 8, on the other hand, displays typical sum and difference patterns of the feed when the spiral arms are excited from their outer terminal points. Notice that the envelope of the sum and difference modes very nearly overlap each other. This is a desired characteristic for optimum system performance. The difference channel also has a very deep null at the boresight axis. This is a characteristic of the two-channel monopulse technique; ideally the depth of the null should be infinite. The two difference peaks are slightly imbalanced. This is a result of imperfections in the spiral surface and/or errors in the amplitude distribution and phase progression in the excitation networks.

Figure 9 shows the spiral feed mounted in a 7-foot parabolic reflector having an f/D = 0.431 1. Radiation pattern characteristics of this A/RIA system at 1435 MHz and 2300 MHz are shown in Figures 10, 11, 12, and 13. Notice that the first sidelobes are at least 22 db below the sum beam maximum and that the null at boresight is very deep (null depths in excess of 65 db have been measured). An axial ratio of less than 1.5 db and a boresight shift of less than 0.25 degree have been recorded over the entire frequency band extending from 1435 MHz to 2300 MHz.

Design Prediction Table I shows typical design performance criteria for parabolic reflector systems when illuminated by spiral antenna feeds. These criteria are given in relation to wavelength and reflector diameter and are valid for systems having f/D ratios between 0.35 and 0.48.

Conclusions The two-channel monopulse feed system discussed in the. preceding paragraphs has many advantages over conventional monopulse antenna feeds. The spiral radiator, being a planar structure, has minimum movement of its phase center with frequency and polarization. This eliminates a large degree of axial defocusing which could cause increased sidelobe levels and decreased system efficiencies. The circularly symmetric patterns provide nearly equal reflector edge illumination for the sum and difference modes, a fact which optimizes the system performance.

TABLE I

Design Prediction Data

Item	Criteria
Half-power beamwidth	65 x λ/D degrees
Gain*	.43 $(\pi D/\lambda)^2$
First null position	87 x λ/D degrees
Sidelobe level**	20 to 22 db
Boresight stability	2.6 x λ/D degrees

* at-rear of antenna.
** aperture blocking not to exceed 4 percent of aperture area.

The spiral feed is capable of simultaneously receiving two LHC and RHC circularly polarized signals and, when illuminating a 7-foot parabolic reflector, has the following performance characteristics:

- 40 percent overall system efficiency.
- Maximum 22 db sidelobes.
- Dual polarization diversity.
- Null depth greater than 40 db.
- Boresight shift less than 0.25 degree.
- Ellipticity of less than 1.5 db on the boresight axis.

Acknowledgements The feed system described in the preceding paper was developed under the auspices of a subcontract from Bendix Radio Corporation, Towson, Maryland.

Bibliography

J. P. Shelton and Wolfe, “Two-Channel Monopulse System, “ Final Report - Phase II, prepared for NASA under Contract No. NAS-5-2071, 15 April 1963.

R. C. Van Wagoner and E. Carpenter, “System Study of an Advanced Monopulse Antenna System, “ Phase I Report, prepared for NASA under Contract No. NAS-5-9713, 4 December 1964.

R. Yaminy, “Antenna Monopulse Tracking Feed, “ Design Plan Report, prepared for NASA under Contract No. NAS-5-10061, 11 July 1967.

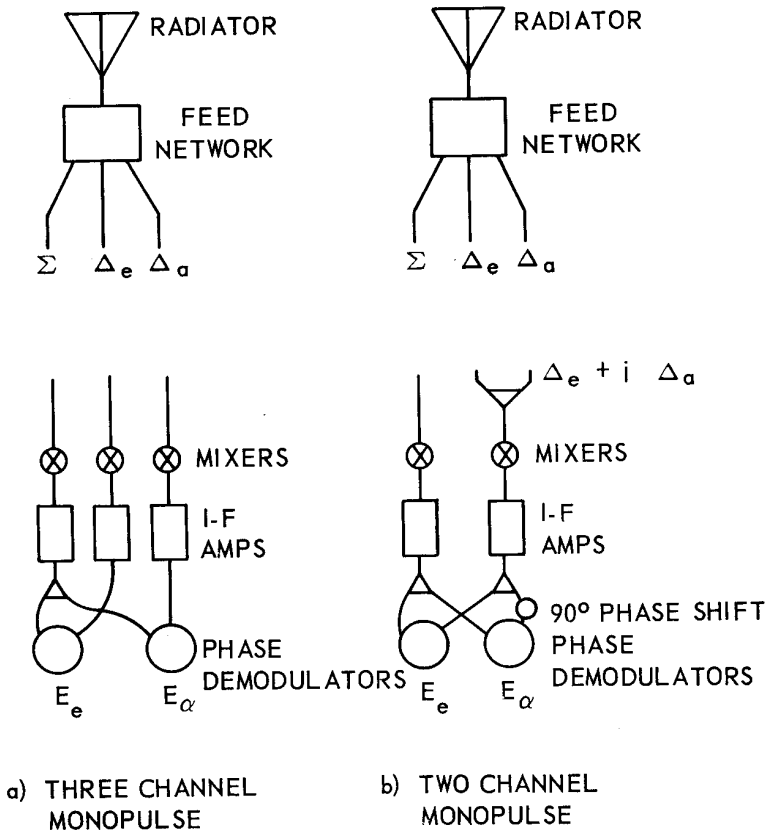

Figure 1. Schematics of Monopulse Systems

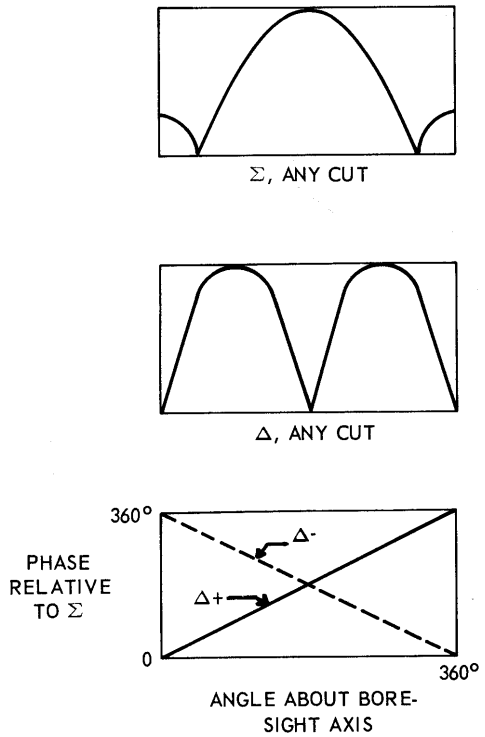

Figure 2. Far Field Two Channel Monopulse Feed Patterns

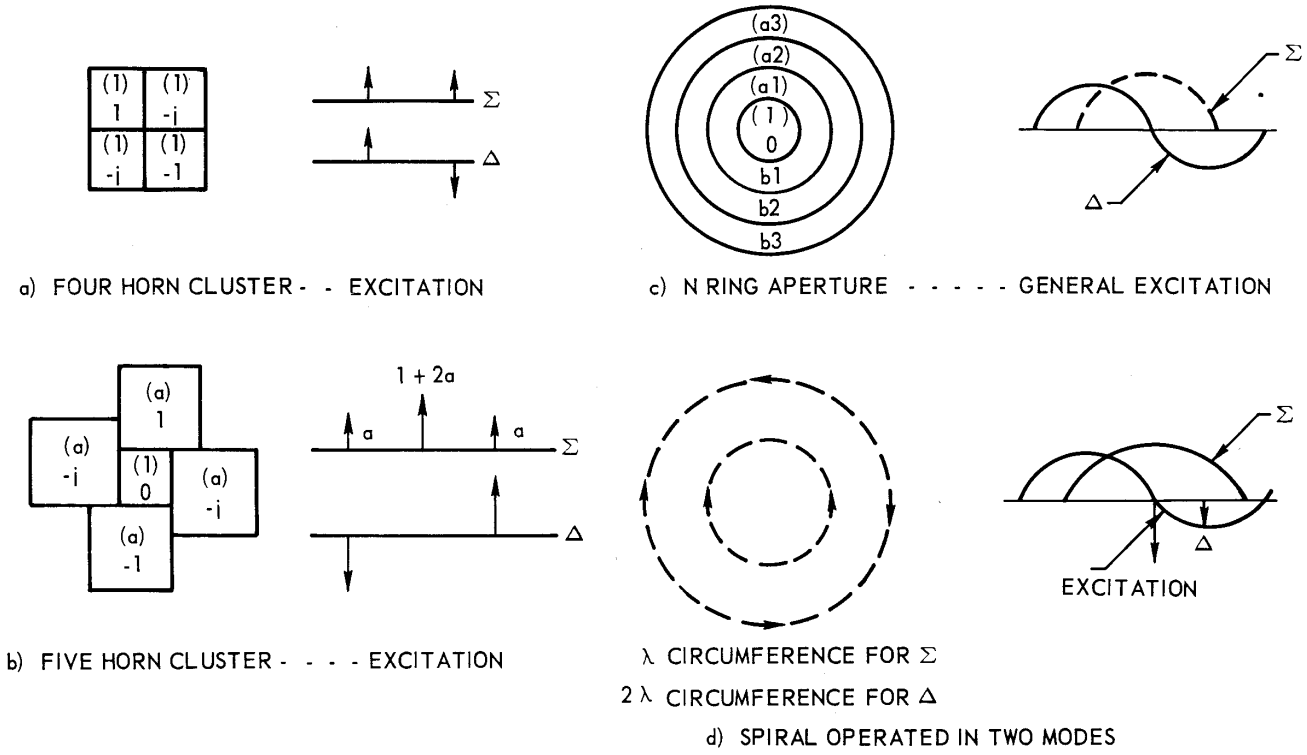

Figure 3. Two Channel Monopulse Aperture Configurations

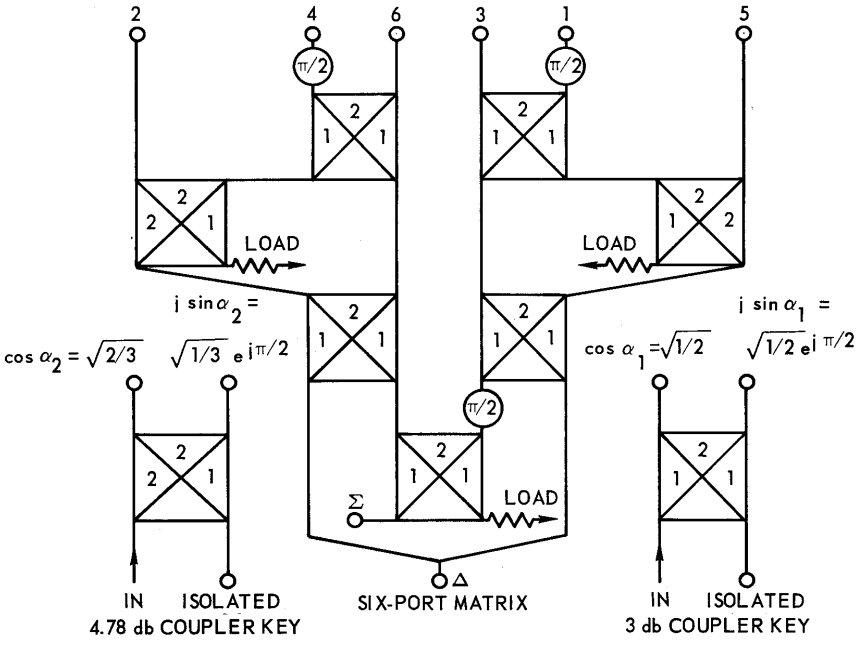

SIX-PORT MATRIX CHARACTERISTICS

CHARACTERISTIC	MODE	PORT					
		1	2	3	4	5	6
AMPLITUDE	Σ and Δ	7.78db	7.78db	7.78db	7.78db	7.78db	7.78db
PHASE	Σ	0°	60°	120°	180°	240°	300°
	Δ	240°	0°	120°	240°	0°	120°

Figure 4. Block Diagram and Electrical Characteristics of Six-Port Matrices

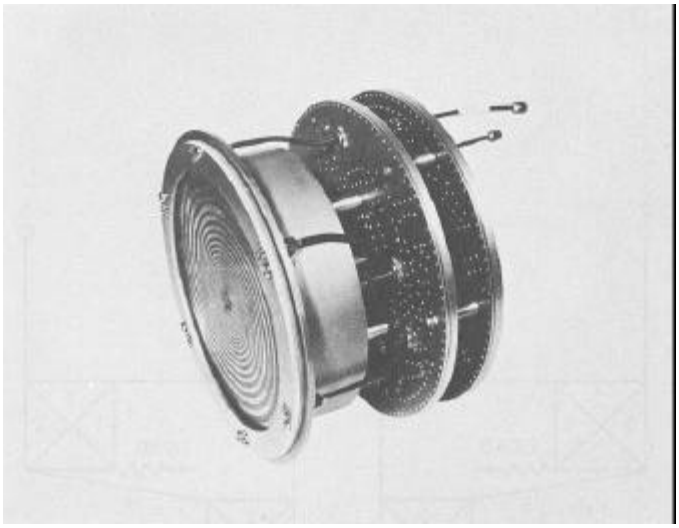

Figure 5. Two Channel Monopulse Antenna

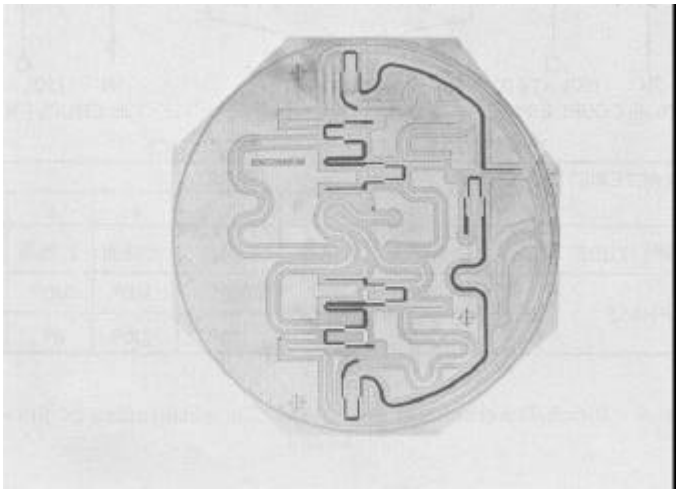

Figure 6. Printed Circuit Comparator Board

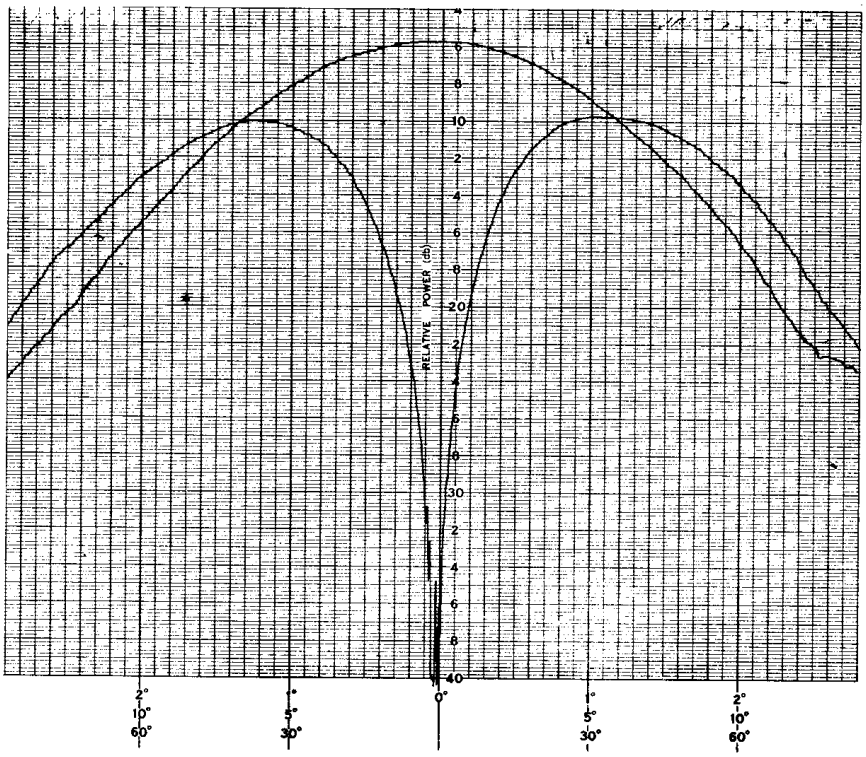

Figure 7. Σ and Δ (LHC) Feed Patterns, 2100 MHz

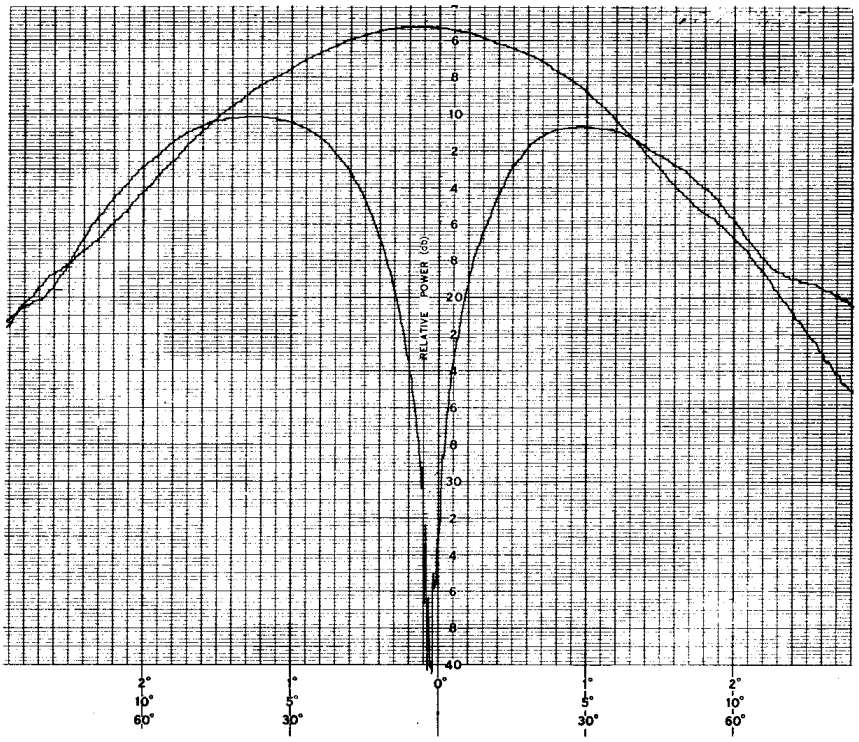

Figure 8. Σ and Δ (RHC) Feed Patterns, 2100 MHz

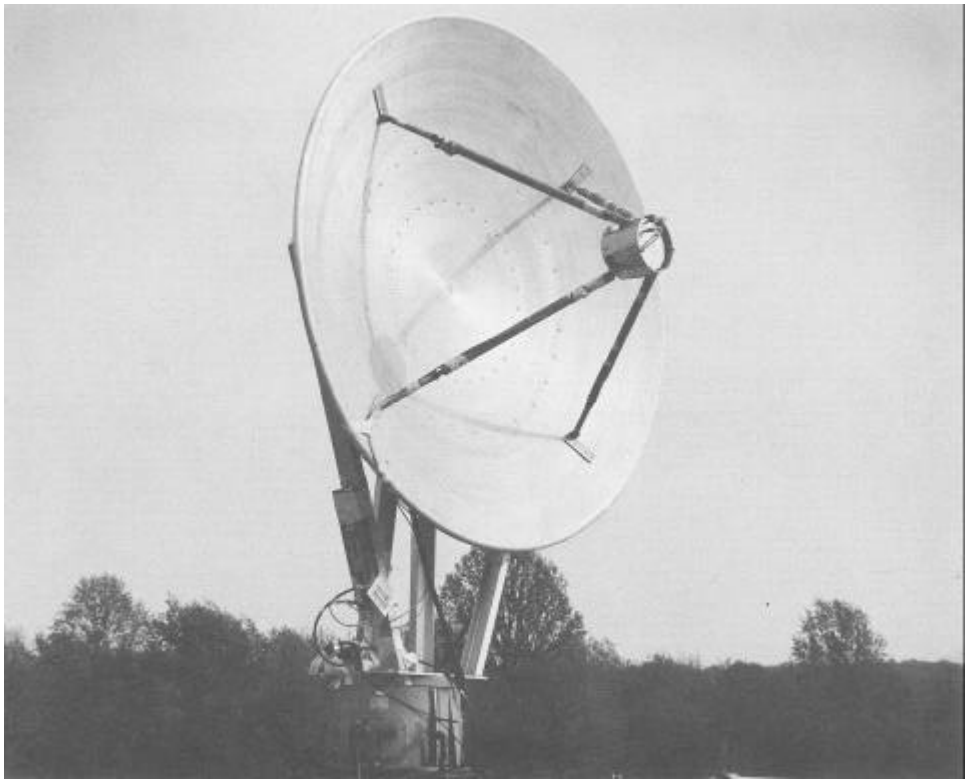

Figure 9. 7-Foot Parabolic Reflector with Spiral Feed

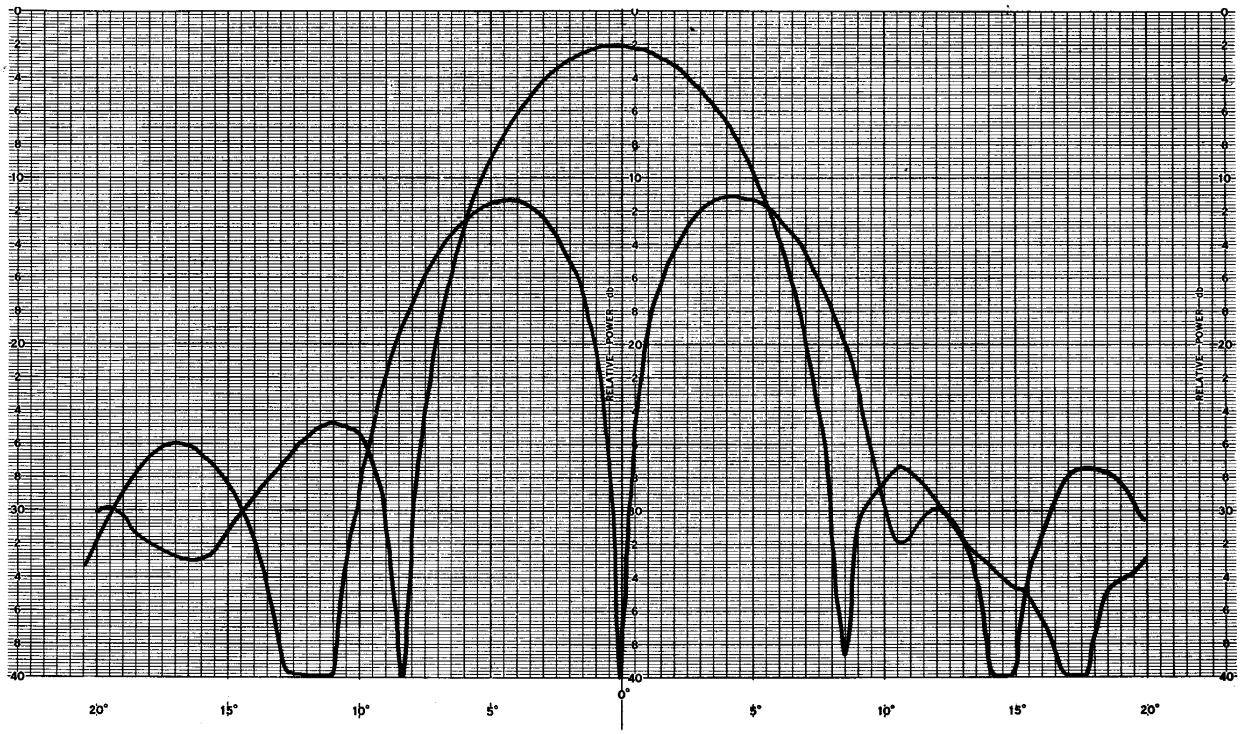

Figure 10. A/RIA Σ and Δ (LHC) Patterns, 1435 MHz

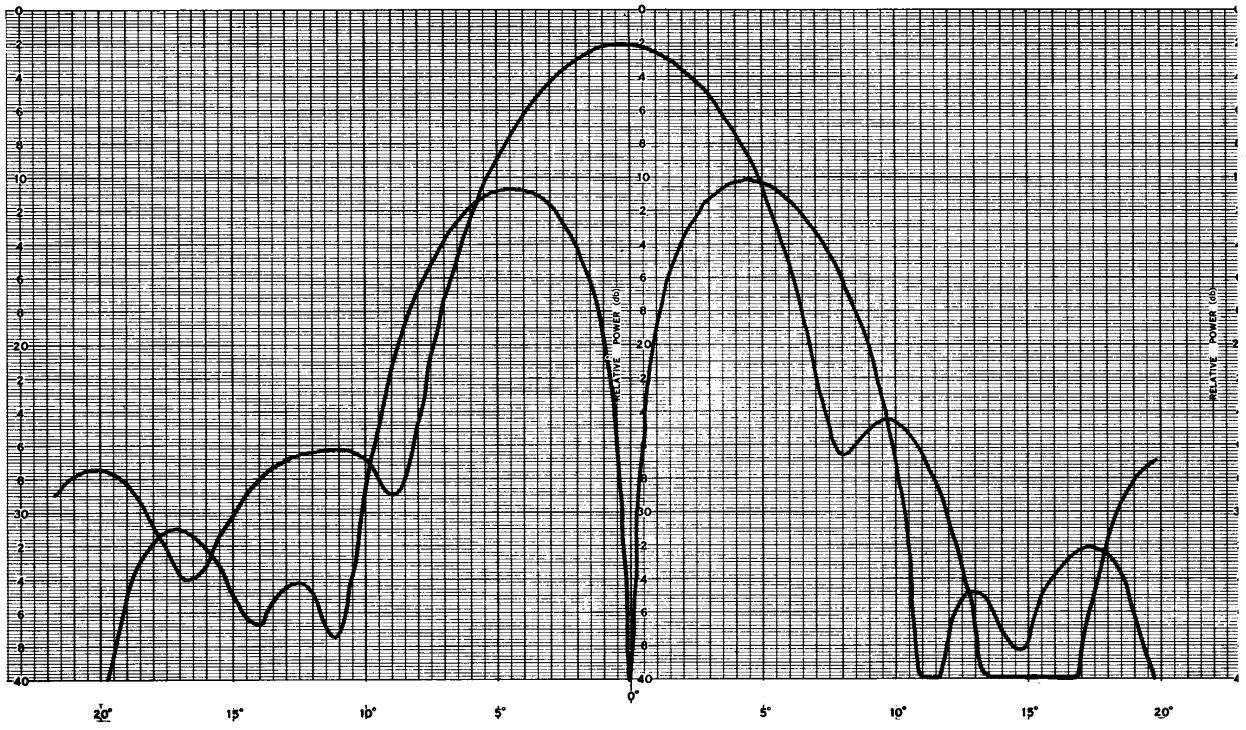

Figure 11. A/RIA Σ and Δ (RHC) Patterns, 1435 MHz

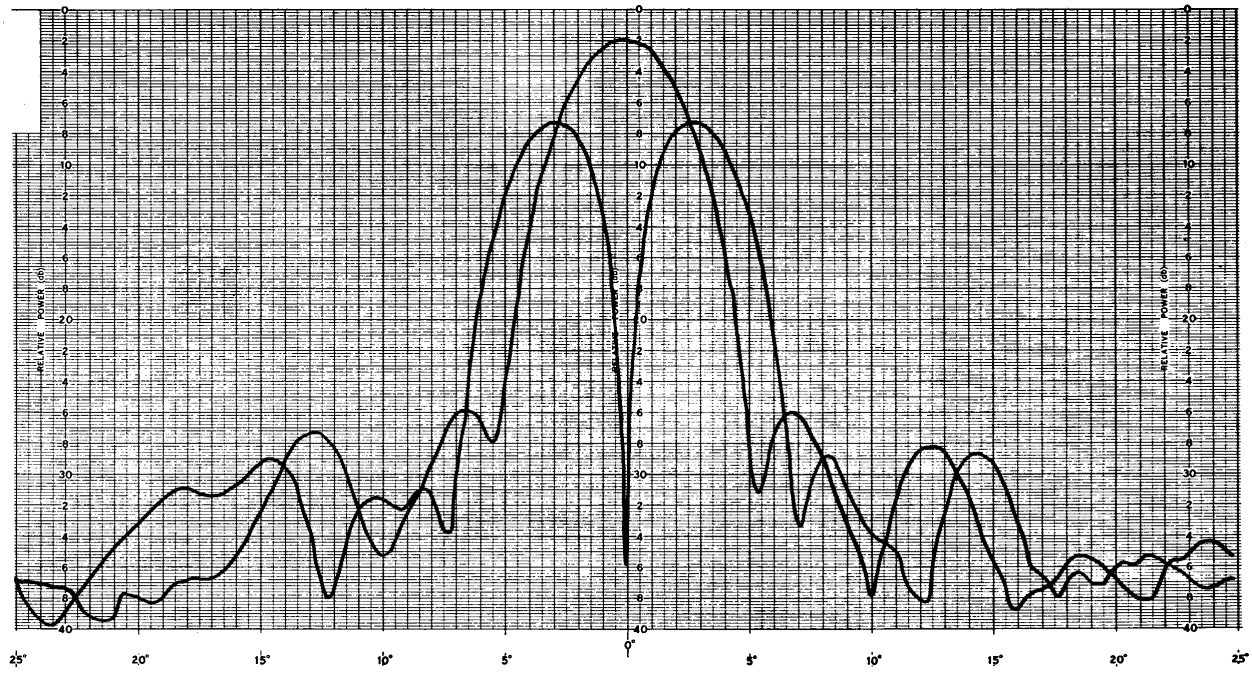

Figure 12. A/RIA Σ and Δ (LHC) Patterns, 2300 MHz

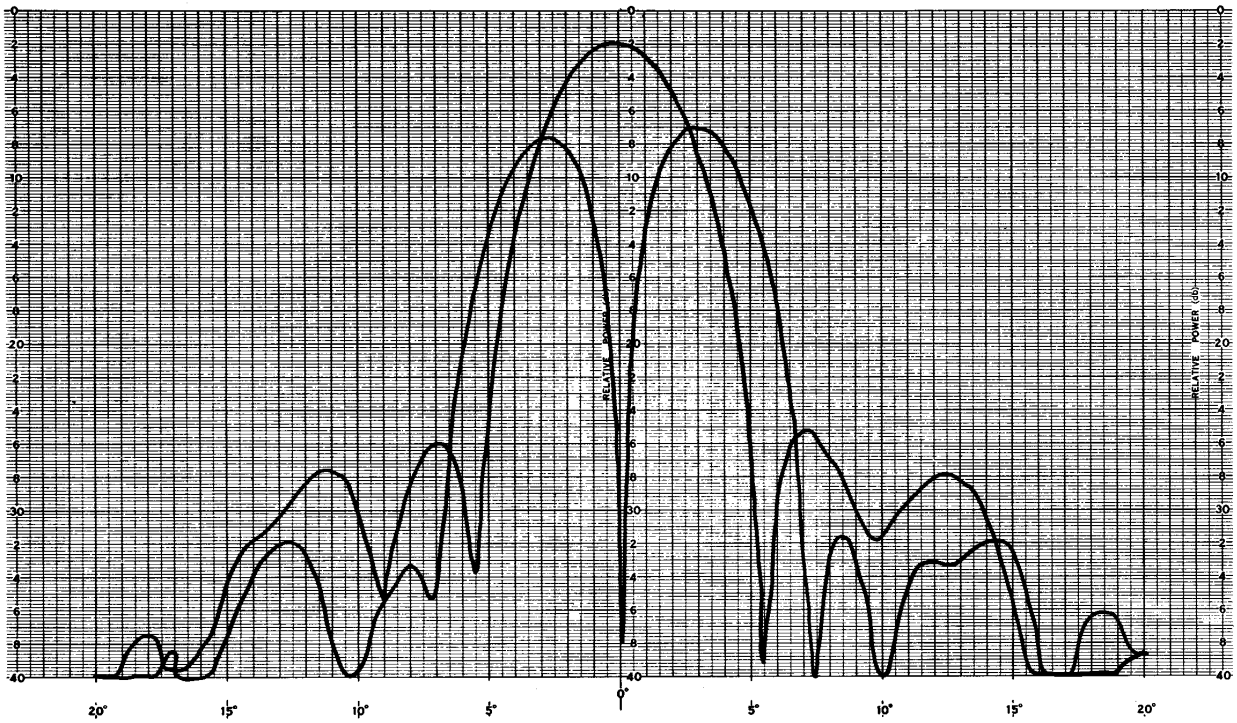

Figure 13. A/RIA Σ and Δ (RHC) Patterns, 2300 MHz